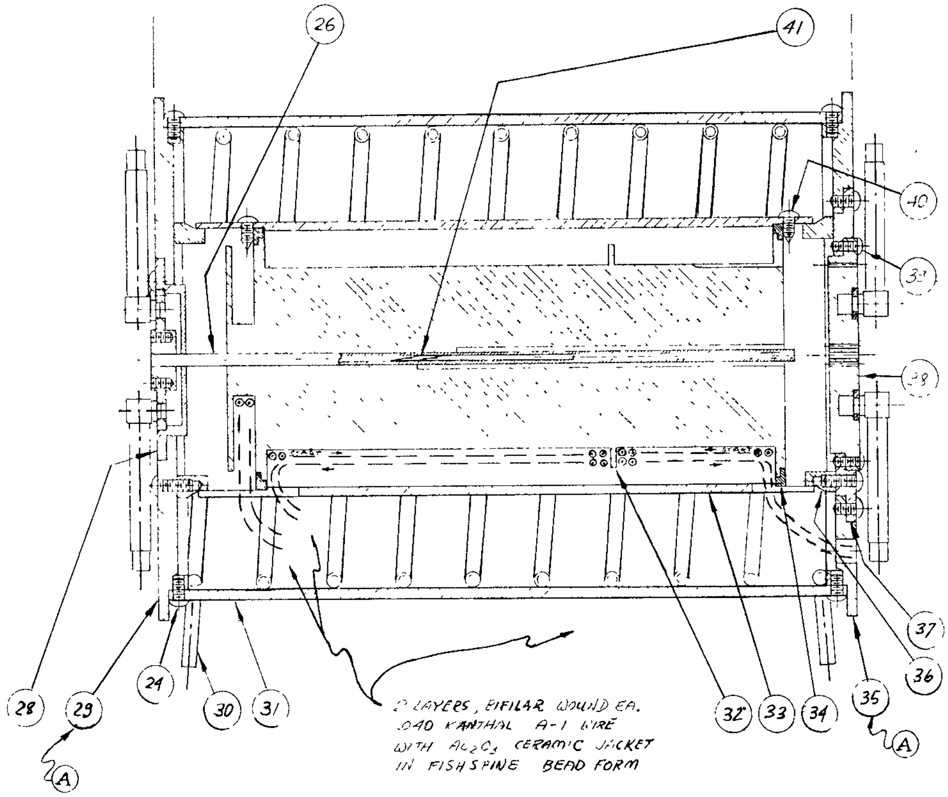

Fig. 3. Assembly drawing of the WR15 noise standard.

the upper one being used as a null detector for the temperature-monitoring potentiometer at the top of the rack.

An assembly drawing of the oven is shown in Fig. 3. The waveguide and termination are items 26 and 41, respectively. The waveguide is manufactured from a platinum 10-percent rhodium alloy to insure a high degree of reliability in predicting its loss characteristics. The termination is a wedge of 40-percent silicon carbide impregnating a beryllium oxide host.

The termination in the waveguide is centered longitudinally in a heat distributor (item 32) to insure a uniform temperature along the termination. The three heating coils (not shown in the drawing) that are wound onto the heat distributor are constructed from a resistive wire stock (5.5 Al, 22 Cr, 0.5 Co, balance Fe) that is considerably more resistant to oxidation than the wire used in previous noise standards [5]. An insulating material (not shown in the drawing) is packed between the heating coils mounted on the heat distributor and the heat distributor sleeve (item 33). The insulating material used is a felt form of zirconium oxide that has an extremely low thermal conductivity. Cooling coils (item 30) are pressed against the inner circumference of the outer casing (item 31) of the oven, and the waveguide flange is cooled by a water jacket (item 28).

ACKNOWLEDGMENT

The author wishes to thank W. F. Foote and E. Campbell, whose design and fabrication efforts were indispensable to the completion of this work.

REFERENCES

[1] "Calibration and test services of the National Bureau of Standards," U. S. Dep. Commerce, Nat. Bureau of Standards, Boulder, Colo., NBS Special Publ. 250.
[2] D. R. Boyle, F. R. Clague, G. R. Reeve, D. F. Wait, and M. Kanda, "An automated precision noise figure measurement system at 60 GHz," *IEEE Trans. Instrum. Meas.* (*1972 Conference on Precision Electromagnetic Measurements*), vol. IM-21, pp. 543-549, Nov. 1972.
[3] W. C. Daywitt, W. J. Foote, and E. Campbell, "WR15 thermal noise standard," Nat. Bureau of Standards, Boulder, Colo., Tech. Note 615, Mar. 1972.
[4] C. T. Stelzried, "Temperature calibration of microwave thermal noise sources," *IEEE Trans. Microwave Theory Tech.* (*1964 Symposium Issue*), vol. MTT-13, pp. 128-130, Jan. 1965.
[5] J. S. Wells, W. C. Daywitt, and C. K. S. Miller, "Measurement of effective temperature of microwave noise sources," *IEEE Trans. Instrum. Meas.*, vol. IM-13, pp. 17-28, Mar. 1964.

Metrological Application of a Stationarity Property in Rectangular Cavities Containing a Dielectric Slab

CHRISTIAN E. EUGENE, MEMBER, IEEE

***Abstract*—A stationarity property for the resonant frequency of a rectangular cavity as a function of the thickness of a low-loss dielectric slab inserted within is used for the accurate determination of the microwave permittivity of the sample. The accuracy estimated to a few promille in X band has been confirmed by experimentation on a standard material.**

I. INTRODUCTION

It is well known that the cavity methods are considered among the best for the accurate measurement of the microwave parameters of dielectric materials. The use of a rectangular cavity containing a dielectric slab has already been reported as a possible structure for such a measurement [1], [2], but until now the most widely recommended configuration remains the cylindrical cavity loaded by an axial-dielectric rod [3], [4]. The use of a stationarity property encountered in the rectangular structure quoted above has given promising results and should revive a new interest in this method.

The basic idea of this stationarity property—which according to us has not yet been considered in the literature—can be explained as follows. A rectangular cavity is considered (Fig. 1), which contains a centrally located dielectric slab (filling the xy section) and which resonates in a TE_{mop} mode; the electric field is thus parallel to the y axis and remains constant along this direction. The sample has a relative permittivity ϵ_r and is assumed to be homogeneous, isotropic, and weakly lossy. For the modes with the third index $p \geq 3$, there is, on each side of the xy median plane, at least one xy plane on which the electric field vanishes. Consequently, if this plane is close to the dielectric interface, the resonant frequency of the cavity will not change at the first order as a function of the sample thickness. It is this stationarity property that will be used below.

Manuscript received May 21, 1973; revised August 6, 1973.
The author is with the Department of Electrical Engineering, Université Catholique de Louvain, Louvain-la-Neuve, Belgium.

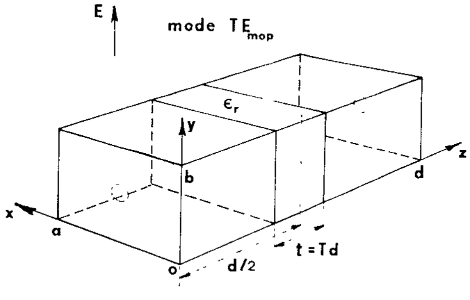

Fig. 1. Rectangular cavity with the centrally located dielectric slab (the coupling holes are shown).

II. Characteristic Relations at a Stationary Point

As already mentioned, the solution for the structure considered above is known and the eigenvalue equation as well as the field expressions are available in analytical form (see also [5]). These relations, presently given in a normalized form, are as follows.

Eigenvalue Equation

$$\frac{\tan X}{X} = \pm \frac{T}{1-T} \frac{(\cot Y)^{\pm 1}}{Y} \tag{1a}$$

with

$$X = \frac{\pi}{2}(1-T)\sqrt{F^2 - A^2}$$

$$Y = \frac{\pi}{2} T\sqrt{\epsilon_r F^2 - A^2}, \quad T = t/d, \quad A = md/a, \quad F = 2df\sqrt{\epsilon_0\mu_0}. \tag{1b}$$

The signs appearing in this multisolution transcendental equation will be plus or minus whether the mode is odd or even, respectively, for the p index.

Electric Field Expressions

$$\bar{E} = E_y(x, z) = f(z) \sin m\pi x/a \tag{2a}$$

with, on the left air part (the situation is symmetric for the right air part),

$$f(z) = \sin \frac{2Xz}{(1-T)d} \tag{2b}$$

and, on the dielectric part,

$$f(z) = \frac{T}{1-T}\cdot\frac{X}{Y}\cos X \sin \frac{2Y}{Td}\left(z - \frac{1-T}{2}d\right) + \sin X \cos \frac{2Y}{Td}\left(z - \frac{1-T}{2}d\right). \tag{2c}$$

The condition $E=0$ introduced at the two dielectric interfaces leads to the characteristic relations at a stationary point (this point will be noted with subscript s for each related quantity). One thus obtains the following *stationary formulas* which happen to be very simple:

$$F_s = \sqrt{A^2 + [2k/(1-T_s)]^2} \tag{3a}$$

$$\epsilon_{rs} = \frac{A^2 + (k'/T_s)^2}{A^2 + [2k/(1-T_s)]^2} \tag{3b}$$

$$\epsilon_{rs} = \frac{1}{F_s^2}\left[A^2 + \left(\frac{k'}{1 - 2k/\sqrt{F_s^2 - A^2}}\right)^2\right] \tag{3c}$$

where the integers k and k' are the number of half-wavelengths of the electric field contained in each of the air portions and in the dielectric portion respectively ($k' = p - 2k$).

The stationarity phenomenon appears clearly in Fig. 2. In this example a cavity is considered that is resonating in the mode TE$_{mo3}$ with $m = a/d$ or $A = 1$. The F-T curves calculated by means of the eigenvalue equation (1) are plotted for different values of ϵ_r. Superposed on these is the stationary F_s-T_s curve (3a) that crosses the former at an inflexion point with horizontal tangent.

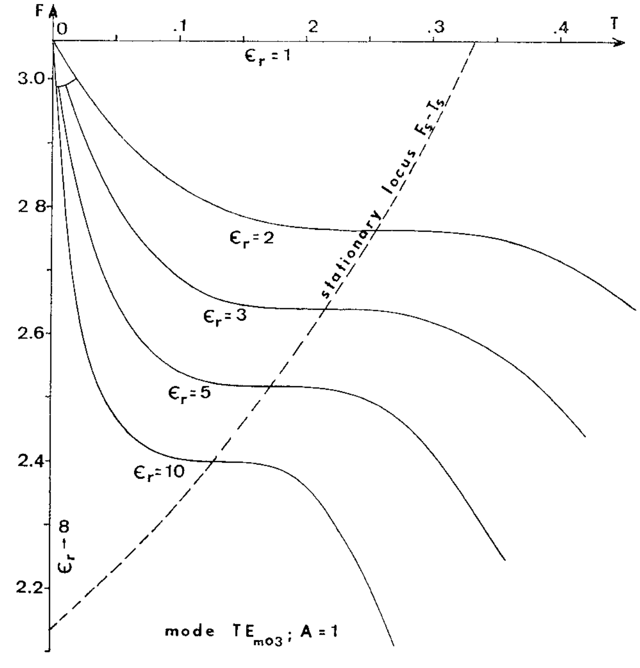

Fig. 2. An example of F-T curves (the stationary locus is shown).

From this stationarity property, two methods of determining the permittivity of the sample were developed as explained hereafter.

III. First Method: Determination of the Permittivity by Frequency Measurement in the Vicinity of a Stationary Point

The most evident practical consequence of the existence of stationary points is that the eigenvalue equation can be solved around such a point with large tolerance for the sample thickness, though without appreciable error for ϵ_r. By expanding this equation in Taylor series around a stationary point and by limiting it at the first nonvanishing term, a cubic dependence of the error on the tolerance is obtained:

$$(\partial\epsilon_r/\epsilon_r)_s = -\frac{\pi^2(\epsilon_r F_s^2 - A^2)}{6\epsilon_r F_s^2}\left[k'^2 - \left(\frac{2kT_s}{1-T_s}\right)^2\right](\partial T/T)_s^3. \tag{4}$$

This expression enables one to determine the admissible tolerance over the sample thickness corresponding to a given error for ϵ_r.

By using the eigenvalue equation (1), the accuracy on ϵ_r still depends on the accuracy with which the measured frequency and the geometrical dimensions of the cavity are known. This dependence is now linear at the first order and one can define a sensitivity factor in the classical way:

$$S_p = \left(\frac{\partial\epsilon_r/\epsilon_r}{\partial p/p}\right)_s \tag{5a}$$

where p is the parameter under consideration. One obtains

$$S_f = -2\left[1 + \frac{2kk'^2}{\epsilon_r(\sqrt{F_s^2 - A^2} - 2k)^3}\right] \tag{5b}$$

$$S_a = -\frac{2A^2}{\epsilon_r F_s^2}\left[1 + \frac{2kk'^2}{(\sqrt{F_s^2 - A^2} - 2k)^3}\right] \tag{5c}$$

$$S_d = S_f - S_a. \tag{5d}$$

As an example, using (4) and (5) one has calculated the tolerances for the geometrical dimensions that would cause an error of 1 percent for ϵ_r when the cavity is constructed with a standard waveguide for X band. The results are given in Fig. 3 as a function of ϵ_r. One observes that the tolerances for a and d are often a few hundredths of millimeters which can be considered very critical. Furthermore the relative uncertainty of the frequency causing the same error is of a few parts in ten thousands; this is more severe than the accuracy obtainable with most of the commercial cavity wavemeters.

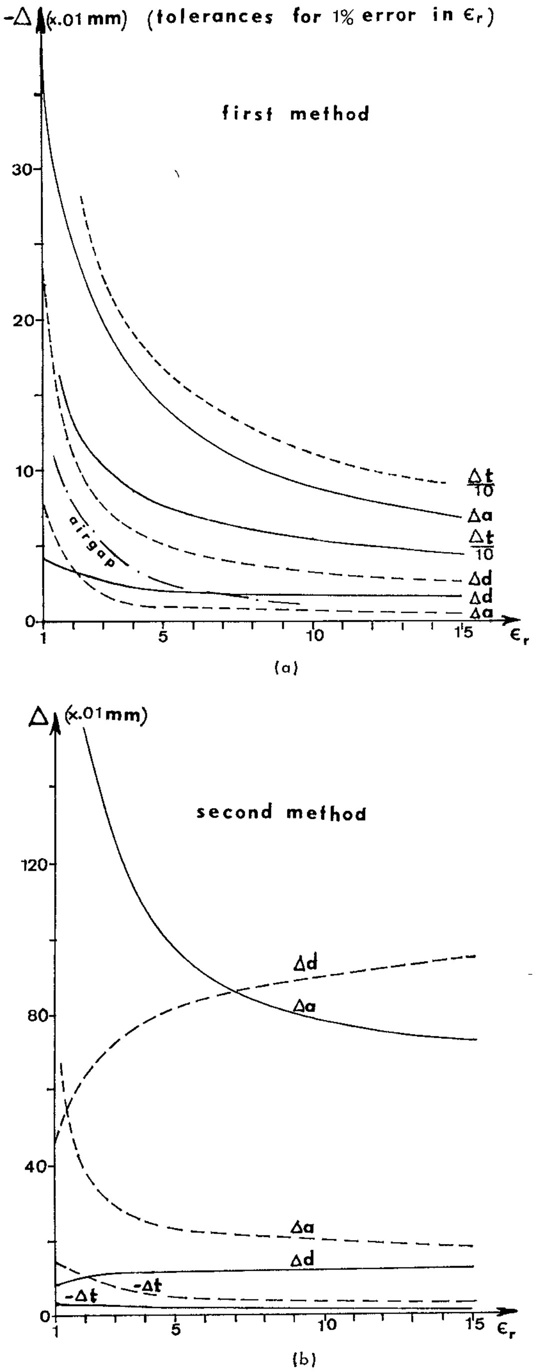

Fig. 3. An example of tolerances for the geometrical dimensions giving an error of 1 percent for ϵ_r by the two methods. Mode TE_{m03}, X-band cavity ($a = 0.9$ in). Solid line: $A = 1$; broken line: $A = 3$.

A last limiting effect to take into consideration is the presence of airgaps between the sample and the metallic walls perpendicular to the electric field. Such airgaps reduce the resonant frequency with respect to its theoretical value. In order to investigate this problem, the classical perturbation method [6] was used. The following result was found for the frequency shift due to a total airgap of βb (b being the height of the cavity). It appeared in close agreement with experimentation.

$$\frac{df}{f} \cong \frac{2\beta\epsilon_r(\epsilon_r - 1)T_s^3(k/k')^2}{(1 - T_s)^3 + 4\epsilon_r T_s^3(k/k')^2}. \tag{6}$$

This frequency shift corresponds ultimately to an uncertainty of ϵ_r. Applying (5b) and (3a) to (6), the following expression is found for the sensitivity factor S_β due to the airgap:

$$S_\beta = \left(\frac{\partial\epsilon_r/\epsilon_r}{\beta}\right)_s = -(\epsilon_r - 1). \tag{7}$$

In the example of Fig. 3, the tolerance for the airgap is also given and once again appears very critical.

Fortunately, this airgap problem can be satisfactorily solved by *metallizing* the dielectric walls facing the gaps. Indeed, if a metallic continuity with the cavity walls may be assumed at the edge of the faces, one is brought back to a case of wall perturbation. Then one states that, for the stationary thickness of the slab, the metallic boundary conditions of the electric and magnetic fields are met at the perturbed walls with the unperturbed fields. Hence there is no perturbation from an electric point of view.

IV. Second Method: Determination of the Permittivity by Solving the $\epsilon_{rs} - T_s$ Formula at a Stationary Point

The stationarity property is used here in a different way which gives more favorable results concerning the influence of the parameters involved. This method consists of determining the stationary thickness of the sample and then deriving the permittivity from the stationary formula $\epsilon_{rs} - T_s$ (3b). A first advantage is that the frequency no longer plays a role. Concerning the sensitivity factors, defined as in (5), the following expressions apply.

$$S_a = \frac{2(\epsilon_r - 1)}{1 + (k'/AT_s)^2} \tag{8a}$$

$$S_t = -\frac{2}{1 + (AT_s/k')^2}\left[1 + \epsilon_r\left(\frac{2k}{k'}\right)^2\left(\frac{T_s}{1 - T_s}\right)^3\right] \tag{8b}$$

$$S_d = -(S_a + S_t). \tag{8c}$$

The numerical results corresponding to the example above are also given in Fig. 3. For the cavity dimensions the situation appears much more favorable than with the previous method. The case of the sample thickness is, however, more critical and requires at least a careful machining of the sample.

This point also raises the problem of precise determination of the stationary thickness. The procedure proposed derives from the remarkable property that, for this stationary thickness, the frequency does not change with any shift of the slab from the center. Indeed there is, in this case, an integer number of half-wavelengths in the slab which therefore acts as a transformer of ratio 1/1 for any position in the cavity. If now the sample thickness deviates from its stationary value, the frequency shift due to slab eccentricity is no longer null and becomes

$$df/f \cong -C\theta\delta^2 \tag{9a}$$

with $\theta = dt/t_s$, $\delta = 2e/(d - t)$, and where e is the slab eccentricity

$$C = \frac{k^2\pi^2\left[\dfrac{1 - T_s}{4T_s}\left(\dfrac{k'}{k}\right)^2 - \dfrac{T_s}{1 - T_s}\right]}{1 + \dfrac{A^2(1 - T_s)^2}{4k^2} + \dfrac{T_s}{1 - T_s}\left(1 + \dfrac{A^2T_s^2}{k'^2}\right)} \text{ (always positive)}. \tag{9b}$$

This result derives from the eigenvalue equation for the uncentered slab (see [1], [5]). Equation (9) enables one to know T_s from a measured frequency shift, provided that the actual thickness is not far from T_s (in the expression of C the yet unknown value of T_s is replaced by an estimate). An alternative way is to consider two successive thicknesses and to use the proportionality between df/f and θ at constant δ.

In the same way as above, the airgaps were considered because they affect the validity of (9). The conclusion of this study is that the effect is very critical and practically the same as with the first method. Here also the solution of metallization is successful for reasons similar to those above.

V. Measurement Results on a Standard Sample

The two methods described in this paper were experimented on a standard sample of high-purity synthetic fused silica, inserted in a $d = 3a$ X-band cavity resonating in the mode TE_{103}. The sample was metallized on two faces by a thin deposition of aluminum.

The results obtained by the two methods are given in Table I. The main limitation with the first method is due to the uncertainty of the frequency (measured in our case by a cavity wavemeter and still corrected for Q factor and coupling holes effects) and to a lesser degree to the warping effects of the cavity. The second method ap-

TABLE I

EXPERIMENTAL RESULTS FOR ϵ_r OF A STANDARD FUSED SILICA SPECIMEN

First Method	Second Method	Value Assessed by Other Lab[a]
3.81_4 (1 ±1.3 percent)	3.81_6 (1 ±0.3 percent)	3.82_4 (1 ±0.1 percent

[a] Laboratory for Insulation Research, M.I.T.

pears more favorable and in close accordance (0.2 percent) with the value assessed by the laboratory which provided the standard material. The limiting factors here are the tolerance for the sample thickness due to machining, and the uncertainty of the stationary thickness inherent in the measuring method.

VI. Conclusions

Examining the performances obtained by the methods used in national laboratories [7], we are tempted to conclude that, for the determination of the permittivity of a low-loss material, our second method is practically comparable to the best methods in use. A study is presently in progress to extend the method to the determination of losses.

Acknowledgment

The author wishes to thank Prof. A. Vander Vorst and Prof. P. Delogne of the Université Catholique de Louvain for useful discussion. He is also indebted to Dr. W. B. Westphal of M.I.T., who kindly supplied him with the standard materials.

References

[1] R. Collin, *Field Theory of Guided Waves*. New York: McGraw-Hill, 1966, ch. 6.
[2] H. Altschuler, "Dielectric constant," in *Handbook of Microwave Measurements*, vol. II, M. Sucher and J. Fox, Ed. Brooklyn, N. Y.: Polytechnic Press, 1963, ch. 9.
[3] F. Horner *et al.*, "Resonance methods of dielectric measurement at centimeter wavelengths," *J. Inst. Elec. Eng. (London)*, vol. 89, pp. 53–68, 1946.
[4] H. E. Bussey and J. E. Gray, "Measurement and standardization of dielectric samples," *IRE Trans. Instrum.*, vol. I-11, pp. 161–165, 1962.
[5] F. Gardiol, "Higher-order modes in dielectrically loaded rectangular waveguides," *IEEE Trans. Microwave Theory Tech.*, vol. MTT-16, pp. 919–924, Nov. 1968.
[6] R. Harrington, *Time-Harmonic Electromagnetic Fields*. New York: McGraw-Hill, 1961, ch. 7.
[7] H. Bussey *et al.*, "International comparison of dielectric measurements," *IEEE Trans. Instrum. Meas.*, vol. IM-13, pp. 305–311, Dec. 1964.

Letters

Possible Mechanisms for the Biomolecular Absorption of Microwave Radiation with Functional Implications

JAMES R. RABINOWITZ

***Abstract*—A theoretical analysis of several possible modes of molecular absorption of microwave radiation suggests that interference with some stereospecific biomolecular processes may result from microwave irradiation.**

Introduction

A physical model on the molecular level of the absorption of microwave radiation, the structural changes that may result, and the relationship of these changes to biomolecular function are important for both analyzing the existing experimental information and designing new experiments that are likely to be informative. As a first step towards constructing such a model, the modes of molecular excitation in the microwave region and their possible effects on biological processes are considered here, using the insights of theoretical molecular physics.

At normal biological temperatures, the number of background photons in the microwave portion of the spectrum is very small, and in a nonirradiated system the only excitations in this energy range are induced by collision. Microwave irradiation is then unlikely to have any direct functional effect on molecules or parts of large molecules that in normal biological circumstances undergo a large number of collisions. In the interior of large molecules, essentially free from collisions, microwave irradiation can cause excitations that will occur only infrequently in nonirradiated systems [1].

The excitations that can result from the absorption of a microwave photon with an energy of 10^{-3}–10^{-6} eV may be divided into three general categories—excitations of: 1) magnetic and electric nuclei–electron coupling states; 2) molecular free rotational states; and 3) constrained motional states of molecular segments (both rotational and vibrational, although at these energies rotational states are much more likely to be important).

1) Magnetic and electric nuclei–electron coupling states are due to the interaction of unpaired electrons with magnetic nuclei, in the former case, and the interaction of nuclear quadrupole moments with the molecular charge distribution, in the latter case. Excitations of these modes do not cause changes in molecular structure, and if biomolecular functions are affected, the mechanism is obscure.

2) Molecular free rotational states are a function of the mass distribution of the molecule. These excitations leave molecular structure unchanged but increase the rotational kinetic energy of the absorber. A large amount of the microwave radiation incident on a biological system is absorbed in this way because water and other small biomolecules have rotational states in the microwave region of the spectrum. While these excitations are biologically important because the local kinetic energy and then the total kinetic energy of the system is increased by collision, their effect is likely to be a result only of the increase in kinetic energy.

3) Constrained motional states are rotational or vibrational states of part of a molecule that leave covalent molecular structure unchanged. For vibrational motion the states are only in the microwave region when tunneling is important. The ammonia molecule provides the classic example of this type of excitation [2]. The rotational states are much more important in the context of this letter because they are more generally in the microwave region.

Parts of molecules, from the size of OH groups up to a number of amino acids, are often free to rotate, constrained by existing covalent bonds. The relative orientation of these molecular segments to the remainder of the molecule is determined by the weak electrostatic interaction potential between the segment and its environment (generally the remainder of the molecule). Although the relative depths of the minima, heights of the barriers, and distances between minima are highly dependent on the segment we are considering and its chemical environment, the potentials are in general multiwell functions, and Fig. 1 is a characterization of such a potential. Depending on the number of constraints, the potential may be more than one dimensional. Similar potentials have been found for simple molecules and ions in solids [3], [4].

The absorption of a microwave photon by the molecular segment would increase its rotational energy. This increase in energy may have two effects that are significant. The segment may now be in a state that is localized in more than one potential well, like states C and D, and reemission of a photon may result in its rotation being localized in a well different from the initial well. Or the segment may be excited to a state like B, still confined to the same single potential

Manuscript received May 14, 1973; revised August 6, 1973.
The author is with the Institute of Environmental Medicine, New York University Medical Center, New York, N. Y. 10016.